Investigation of Fast Pitch Angle Scattering of Runaway Electrons in the EAST Tokamak

H. W. Lu[1,2], L. Q. Hu[2], S.Y. Lin[2], R. J. Zhou[2], J. R. Luo[1], F. C. Zhong[1] and EAST Team

[1]Department of Applied Physics, Donghua University, Shanghai 201620, P.R. China

[2]Institute of Plasma Physics, Chinese Academy of Sciences, Hefei 230031, P.R. China

Abstract

An experimental study of the investigation of fast pitch angle scattering (FPAS) of runaway electrons in the EAST tokamak has been performed. From the newly developed infrared detector (HgCdTe) diagnostic system, the infrared synchrotron radiation emitted by relativistic electrons can be obtained as a function of time. The FPAS is analyzed by means of the infrared detector diagnostic system and the other correlative diagnostic systems (including electron cyclotron emission, hard x-ray, neutrons). It is found that the intensity of infrared synchrotron radiation and the ECE signal increase rapidly at the time of FPAS because of the fast increase of pitch angle and the perpendicular velocity of the energetic runaway electrons. The Parail and Pogutse instability is a possible mechanism for the FPAS.

Keywords: runaway electron beam, instability, fast pitch angle scattering (FPAS), tokamak

PACC: 5235P, 5270L, 5260

1. Introduction

In the tokamak concept the confinement of the plasma is achieved by driving a current through the plasma column [1]. This plasma current is generated by an

inductive electric field in the toroidal direction. The presence of this electric field leads to the phenomenon of electron ‘runaway’ [2]. In the electric field, electrons which exceed a critical velocity, for which the collisional drag balances the acceleration by the field, are accelerated freely and can reach very high energies [3]. In low density tokamak discharges a considerable number of runaway electrons can be created, with energies up to tens of MeV. At present, runaway electrons in tokmak plasmas seem to be undesirable especially the high energetic runaway electrons. These can cause severe damage to the vacuum vessel and are a potentially dangerous source of hard X rays. Apart from their unpleasant contribution to the background radiation (hard X-rays, photoneutrons) requiring heavy diagnostic shielding and staff protection as well as interfering neutron ion temperature measurements, runaway electrons can carry a large fraction (~50%) of the plasma energy to the walls in low density discharges and might be a non-negligible energy sink in the currently studied tokamak regimes [4]. On the other hand, runaway electrons can carry a substantial amount of the plasma current and may have beneficial effects on plasma confinement (such as in the slide-away regime) [5]. Therefore, the runaway electrons formation and their consequence on the machine components have been identified as a major issue for ITER operation [6].

The runaway electrons are collisionally decoupled from the bulk plasma, due to high relative velocities and the associated small collision cross-section [1]. In spite of this small collisional interaction there is still interplay between the runaway electrons and the bulk plasma. The mutual influence between collective plasma effects and the

runaway electrons can give rise to several instabilities [7]. Relativistic electrons moving on a curved orbit emit infrared synchrotron radiation. Exploitation of this radiation for the tokmak case provides the possibility to diagnose confined runaway electrons inside the plasma. The first pioneering measurements of this kind were performed at the TEXTOR tokamak by Finken et al [8]. With help of infrared synchrotron radiation diagnostics, the behaviors of runaway electrons beams, including the runaway electron beam instabilities can be investigated in detail.

The Parail and Pogutse instability mechanism is a two stage process [1]: First, if the energy of runaway electrons W reaches some critical value ($W > 9(\omega_{ce}/\omega_{pe})^3 W_{crit}$,where W_{crit} represents the critical energy when electrons to run away), Langmuir waves are excited. Second, a Cerenkov resonance of the electrons on these waves drives a broad spectrum of waves (containing lower hybrid waves, peaking around the ion plasma frequency ω_{pi} [9, 10]). Anomalous Doppler resonance will cause pitch angle scattering of the runaway electrons due to these lower hybrid waves if the resonance criterion ($\omega_k - n\omega_{ce} = k_{//} v_{//}$, ω_k is the frequency of the lower hybrid waves, n is the harmonic resonance, $k_{//}$ is in the parallel direction, $v_{//}$ is the parallel velocity of runaway electrons) is fulfilled. Note that for low densities $\omega_{lh} = \omega_{pi}$, where ω_{lh} is the frequency of the lower hybrid waves.

In low density ohmic discharges almost all detected neutrons are (γ, n) neutrons, created when a runaway electron hits the carbon limiter or when highly energetic X rays hit the lead collimator of the detector [5]. For both processes the incident energy of the photon must exceed 10 MeV. An infrared detector (HgCdTe) diagnostic system

was developed recently to detect the infrared synchrotron radiation emitted by the relativistic electrons confined in the interior of the plasma on the EAST Tokamak. Whereas the hard x-ray diagnostic system and neutron diagnostic system were used to monitor the runaway electrons escaping from the chamber. With the help of correlative diagnostic system, fast pitch angle scattering of runaway electrons confined inside the plasma was investigated in this paper.

This paper is organized as follows. In section 2, the experimental set-up is described. In the next section we present the experimental results and discuss a possible mechanism to explain the observation. Finally, our conclusions are presented in section4.

2. Experimental setup

EAST is a fully superconducting tokamak both in toroidal field (TF) and poloidal field (PF) with noncircular cross-section. It has a major radius of $R_0 = 1.75m$, a minor one of $a = 0.4m$. The superconducting TF magnetic system of EAST consists of a toroidal array of sixteen coils. It produces a 3.5T toroidal field at the plasma major radius of 1.7m. The superconducting PF system of EAST consists of twelve coils located symmetrically above the vertical mid-plane and the equatorial plane. The PF coils provide a 1.0 MA ohmic plasma current with up to 11Vs of inductive flux [11]. In the campaign of 2009, EAST tokamak was normally operated at $I_p = 100 - 800kA$, $B_T = 2T$, central line-averaged density $\overline{n_e} = (0.5 - 5) \times 10^{19} m^{-3}$, $T_e = 0.2 - 2.0keV$, and $T_i = 0.1 - 1.0keV$.

In the EAST tokamak, runaway electrons with energies up to 25MeV have been

observed directly with an infrared detector (HgCdTe, liquid nitrogen cooled, with an area of $0.35mm \times 0.35mm$) system, which measures the synchrotron radiation in the wavelength range $5-13\mu m$. Fig.1 shows a schematic of the set-up used for synchrotron radiation measurements. The detector is positioned to view the plasma in toroidal direction tangentially to the electron forward direction as it is shown in Fig.1. The incoming light is reflected by a mirror and collected via a lens by a HgCdTe detector. The mirror views only a part of the poloidal cross section because of the window limits. Therefore the synchrotron radiation intensity collected by the system is too low in general and only the energetic runaway electrons can be observed by the infrared detector. Its time resolution is several μs. This is sufficient to investigatigate the runaway electrons instability.

3. Experimental results

Fig.2 shows the temporal evolution of various quantities in shot No.12964. The plasma current is fixed at about 250kA. The central line-averaged density is approximately $0.8\times10^{19}m^{-3}$, slightly changing during the discharge. The plasma current and central line-averaged electron density were feedback controlled during the discharges.

As can be seen from Fig.1, there are four sudden infrared synchrotron radiation bursts during the whole discharge. A jump of the ECE signal and enhanced Mirnov oscillations coincide with the jump of infrared synchrotron radiation. The infrared synchrotron radiation signal decays rapidly thereafter, while the ECE signal increases stepwise. The decrease of the infrared synchrotron radiation signal is attributed to

radiative deceleration of runaway electrons. That is to say, runaway electrons are loosing energy by the enhanced synchrotron radiation as a result of the FPAS. The ECE signal begins to decrease when the infrared synchrotron radiation signal falls to the lowest level. One can also see from the figure that the time interval between two FPAS becomes longer and longer because of the loop voltage which is seen to decrease between 2.0 - 7.0 s in Fig.1. This is because it takes more time to accelerate low energy runaway electrons to the critical energy due to the lower electric field.

The stepwise increase of the ECE signal (as shown in Fig.3) at the FPAS agrees with the increase in perpendicular energy of the runaway electrons. The ECE signal shows a multiple step process, while there is only one step in the infrared synchrotron radiation signal. The reason is that the Parail Pogutse instability most pronounced at its first occurrence [1]. This is corroborated by the ECE signal whose first step is the largest in Fig.3. We can see from the same figure that the intensity of step emission became smaller than the step before. The energy density of the excited waves in subsequent instabilities is apparently too low to increase the pitch angle noticeably and thus the perpendicular energy of the runaway electrons. Furthermore, runaway electrons are loosing energy (perpendicular energy and parallel energy) by the enhanced radiation (ECE and IR) as a result of the FPAS.

At the occurrence of the FPAS, the ECE signal shows also features of runaway electron instabiliy as it is shown in Fig 3. We can see from Fig.1 and Fig.3 that after three or four steps the ECE signal start to decrease. The period between the steps is about 10ms-15ms which is comparable with that in TEXTOR (10ms) [1]. However, it

is unlikely that the magnetic field ripple resonance causes the FPAS since the abrupt stop of the process cannot be explained this way. To leave the resonance region for the second harmonic interaction, i.e. to radiate 2 MeV, about 35ms are required [1], much longer than observed (10ms-15ms).

The time during which the infrared synchrotron radiation increases in intensity is $\Delta t = 135\mu s$ which is comparable with that in TEXTOR ($\Delta t = 125\mu s$) [1], as it is shown in Fig.4. For most tokamaks the Parail Pogutse instability is observed to be of the order of $100\mu s$ [12]. The synchrotron radiation intensity can change only by a change in the energy W_r, number N_r or pitch angle θ of the runaway electrons. The short time ($\Delta t = 135\mu s$) excludes a possible energy gain of the runaway electrons or an increase in number Therefore, the change in the pitch angle of the runaway electrons is the only reasonable explaination for the increase of synchrotron radiation on such a short time scale. The transient events observed on the synchrotron radiation which give evidence of rapid changes of the pitch angle represents a runaway instability resulting from the interaction between the runaway electrons and plasma oscillations. Fast Pith Angle Scattering (FPAS) of the relativistic runaway electrons is therefore the only viable explanation of this behavior.

Although a drastic change in the runaway electrons emission is observed during the FPAS, this event does not seem to affect the bulk plasma. No indications of changes in density, loop voltage or plasma current are found (see in Fig.2). However, all runaway sensitive signals such as ECE, IR, HXR and neutron emission confirm the FPAS activity.

Fig.5 shows the trace of emission signal of infrared synchrotron emission emitted by runaway electrons confined inside the plasma whereas hard x-ray emission outside of the vacuum and photo-neutrons are produced by high energetic runaway electrons leaving from the plasma. When the energetic runaway electrons are lost from the plasma, they generate hard x-ray radiation by collision with the plasma facing component (PFC). These hard x-rays can also produce neutrons by photo-nuclear reactions. The PFC in this campaign is made from carbon. The threshold energy for carbon, the limiter material is about 10MeV. The loss of energetic runaway electrons with energy of at least 10MeV is clearly visible on the neutron signal. Note that under the plasma conditions of low density discharges the amount of fusion neutrons is negligible [13]. Therefore, we can see from the Fig.5 that the counts of hard x-rays and photo-neutrons decrease when FPAS happens.

The count rates of hard x-rays in different energy ranges are shown in Fig.6. We can see from the figure that the intensity in the low energy range (1.5-2.0MeV) droops rapidly with the occurrence of the FPAS event, but increases progressively thereafter. This is opposite for the high energy hard x-ray emission (9.5-10.0MeV). There is a sharp increase of the high energy hard x-rays when the FPAS event happens, followed by a decay. The reason is that, for low energy runaway electrons the parallel velocity decreases rapidly and the perpendicular velocity increases fast. The pitch angle θ of low energy runaway electrons increases immediately. Therefore, the electron cyclotron emission increases rapidly. The energy of runaway electrons is reduced to a lower energy (for example, from 1.5-2.0MeV to 50-100keV, shown in Fig 6 and 7).

For the high energetic runaway electrons (20-30MeV), the intensity of infrared synchrotron radiation increases to a high level in a short time ($135\mu s$) due to FPAS. Therefore, the energy of these high energetic runaway electrons is reduced to a lower level (9.5-10.0MeV, see Fig.6). The number of runaway electrons in the energy range of (9.5-10.0MeV) increases immediately after FPAS, and decreases progressively, because of the acceleration of inductive electric field to higher energy (may be several ten MeV).

We can also see from the Fig.6 that the count rate of hard x-ray emission in the energy range of 9.5-10.0MeV is higher than that in the energy range 7.5-8.0MeV, Therefore, there is a high energetic runaway electron beam (several ten MeV) inside of the plasma.

Fig.8 shows three CCD images of shot No.12964 at three different times (360 ms 365 ms and 370 ms). The dust grains are heated by the runaway electrons and a snow shower picture is recorded in Fig.8 at 365 ms. On the photo the visible dust density is thus correlated to the runaway electrons density. There is a runaway electron beam with the radius about 10 cm in the middle of the chamber as it is shown in Fig.8 at 365ms. The bursts of impurity (mainly carbon dust) radiation in the background plasma are associated with the runaway electron and wall interaction which can produce carbon dust. The runaway electron and wall interaction is associated with the Parail and Pogutse instability and FPAS. These events show the transverse transport of runaway electrons towards the first wall.

4. Discussion and Conclusions

The generation rate of the primary runaways depends on plasma density, electron temperature, the ratio $\varepsilon = E_0 / E_c$ (with $E_c = e^3 \ln \Lambda n_e Z_{eff} / 4\pi\varepsilon^2 T_e$, the critical Dreicer field) but doesn't show any dependence on the magnetic field [14]. The only known runaway-related phenomenon exhibiting a sensibility with regard to the magnetic field, is the kinetic instability driven by the runaway electrons [15, 16]. The Parail and Pogutse instability criterion in the longitudinal velocity space is [17]: $v_{beam} > 3v_{cr}(\omega_{ce} / \omega_{pe})^{3/2}$, where $v_{cr} = v_{Te}(E_c / E_0)^{1/2}$. When the velocity of runaway electrons reaches the critical value v_{beam}, the Parail and Pogutse instability is excited. Mirnov oscillations in Fig.2 also show the Parail and Pogutse instability. Thereafter the parallel velocity is transformed into perpendicular velocity because of the interaction between energetic runaway electrons and lower hybrid waves are excited by Cerenkov resonance of the electrons on Langmuir waves. Anomalous Doppler resonance will result in pitch angle scattering of the runaway electrons if the resonance criterion ($\omega_k - n\omega_{ce} = k_{//} v_{//}$) is fulfilled. Therefore, the pitch angle θ of high energetic runaway electrons increases immediately (FPAS). The intensity of infrared synchrotron radiation and the ECE signal increase rapidly at the time of FPAS because of the fast increase of pitch angle and the perpendicular velocity of the runaway electrons.

Neither the two stream instability [7, 18, 19] nor the excitation of a parameter instability [20, 21, 22] or the instability evocated by a positive slope in the distribution function [7] are considered likely to explain the observed phenomena. since the bulk plasma is nearly unaffected by the instability; the FPAS is independent of the number

of high energy electrons [1] and the step-like increase of the ECE signal while the absence of an oscillating character of the infrared synchrotron radiation. It is unlikely that the magnetic field ripple resonance causes the FPAS analyzed above. Therefore, the Parail and Pogutse instability is a possible mechanism for the FPAS.

Acknowledgements

This work has been supported by the National Nature Science Foundation of China, No.10775030 and No. 10775041. This work was supported partly by JSPS-CAS Core-University Program in the field of “Plasma and Nuclear Fusion”. The corresponding author is grateful to all members of the EAST-Team for their contribution to the experiments.

Reference

[1] Jaspers R, 1995 Relativistic runaway electrons in tokamak plasma, PHD Thesis, Eindhoven University of Technology, The Netherland (ISBN 90-386-0474-2)

[2] Knoepfel H, Spong D A, 1979 Nucl. Fusion **19** 785

[3] Jaspers R, Lopes Cardozo N J, Finken K H, 1994 Physical Review Letters **72** 4093

[4] Brossier P, 1993 Nucl. Fusion **18** 1069

[5] Jaspers R, Finken K H, Mank G, 1993 Nucl. Fusion **33** 1775

[6] ITER Physics Basis, 2007 Nucl.Fusion **47** S178

[7] A.B. Mikhailovskii, Theory of Plasma Instabilities, Vol. 1 (Consultans Bureau, New York, 1974)

[8] Finken K H, Watkins J G, Rusbuldt D, 1990 Nucl. Fusion **30** 859

[9] Oomens A A M, Ornstein L Th M, Parker R R, Schuller F C and Talor R J, 1976

Phys.Rev.Lett. **36** 255

[10] Schokker B C, de Vries P C, Oomens A A M, Schuller F C, Lopes Cardozo N J, and RTP-Team, 21st Eur. Conf. on Controlled Fusion and Plasma Physics, Montpellier (1994) I-286

[11] Lu H W, Hu L Q, Chen Z Y, 2008 J.Plasma.Physics. **74** 445

[12] Parail V V and Pogutse O P, Runaway electrons in a Tokamak, in Reviews of Plasma Physics, Vol.11, ed. by M.A. Leontovich (Consultans Bureau, New York, 1986)

[13] Entrop I, 1999 Confinement of relativistic runaway electrons in tokamak plasmas, PHD Thesis, Eindhoven University of Technology, The Netherland (ISBN 90-386-0947-7)

[14] Plyusnin V V, 29th EPS Conference on Plasma Phys. and Contr. Fusion Montreux, 17-21 June 2002 ECA Vol.**26B** (2002) P-4.097

[15] Alikaev V V, Razumova K A, Sokolov Y A, 1975 Plasma Physics Reports, **1** 303

[16] Parail V V, Pogutse O P, 1978 Nuclear Fusion **18** 303

[17] Plyusnin V V, Cabral J A C, Figueiredo H, Varandas C A F, 28th EPS Conference on Contr. Fusion and Plasma Phys. Funchal, 18-22 June 2001 ECA Vol.**25A** (2001) 601-604

[18] Thode L E andSuddan R N, 1975 Phys. Fluids **18** 1552

[19] Breizman B N, Collective Interaction of Relativistic Electron Beams with Plasmas, in Reviews of Plasma Physics, Vol.15, ed. by B.B. Kadomtsev (Consultants Bureau, New York, 1990)

[20] Kaw P K, Kruer W L, Liu C S, Nishkawa K, Parametric Instabilities in Plasma, in Advances in Plasma Physics, Vol.6, ed. by A. Simon, W.B. Thompson (Wiley, New York, 1975)

[21] Papadopoulos K, 1975 Phys.Fluids **18** 1769

[22] Chen F F, Introduction to Plasma Physics and Controlled Fusion, Vol.1 (Plenum Press, New York, 1984)

Figure Caption:

Fig.1. Schematic view of infrared detector (HgCdTe) diagnostics on the EAST Tokamak;

Fig.2. Temporal evolution of some parameters in shot No.12964. From top to bottom: (I_p) the plasma current, (V_{loop}) loop voltage, (Ne) line-averaged density, (IR) infrared synchrotron radiation, (ECE) signal of electron cyclotron emission and (dB/dt) (Mirnov oscillations).

Fig.3 The ECE signal in detail (shot No.12964).

Fig.4 Infrared synchrotron emission in detail (shot No.12964)

Fig.5 Three emission signals in shot No.12964. From top to bottom: infrared synchrotron emission emitted by runaway electrons; hard x-ray emission outside of the vacuum; photo-neutrons.

Fig.6 Count-rates recorded by hard x-ray diagnostics in different energy ranges (shot No.12964)

Fig.7 Count-rates detected by fast electron bremsstrahlung (FEB) diagnostics in different energy ranges (shot No.12964)

Fig.8 Three CCD images of shot No.12964 at times: 360 ms 365 ms and 370 ms

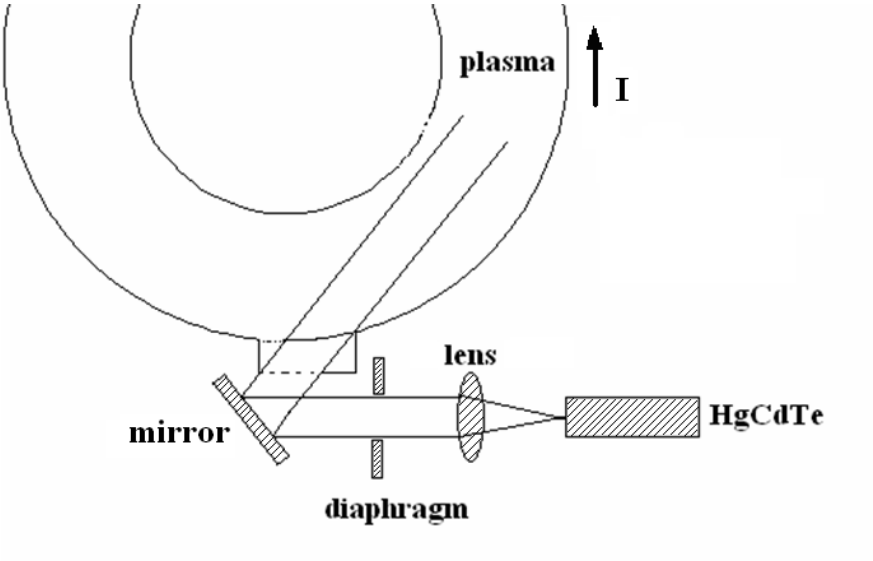

Fig.1

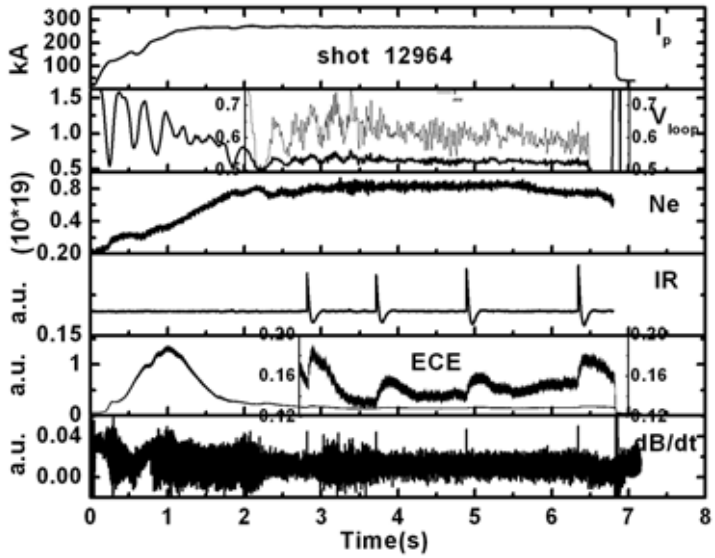
shot 12964
I_p
kA
300
200
100
V
1.5
1.0
0.5
0.7
0.6
0.5
V_{loop}
(10^19)
0.8
0.4
0.20
Ne
a.u.
IR
0.15
0.20
0.16
0.12
ECE
1
0
a.u.
0.04
0.00
dB/dt
0
1
2
3
4
5
6
7
8
Time(s)

Fig.2

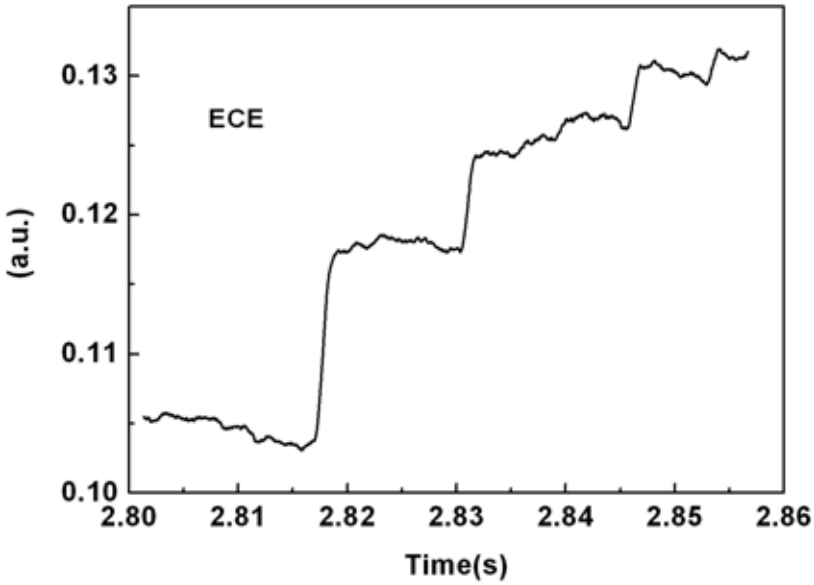

Fig.3

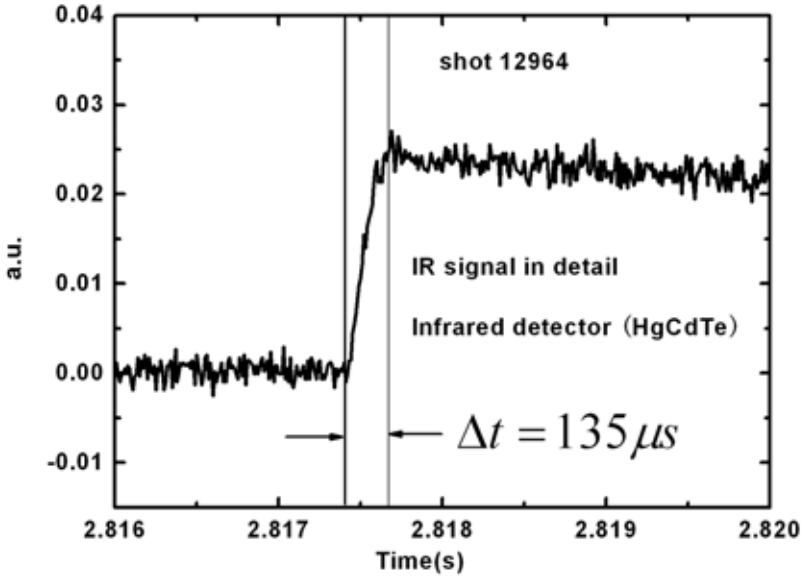
shot 12964
IR signal in detail
Infrared detector（HgCdTe）
$\Delta t = 135\mu s$
a.u.
Time(s)
0.04
0.03
0.02
0.01
0.00
-0.01
2.816
2.817
2.818
2.819
2.820

Fig.4

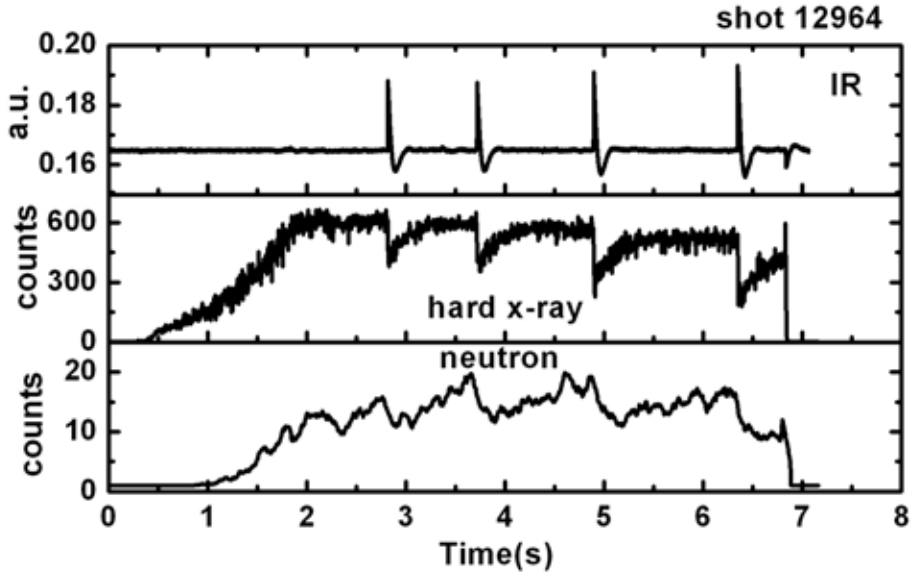
shot 12964
IR
a.u.
0.20
0.18
0.16
counts
600
300
0
hard x-ray
neutron
counts
20
10
0
0
1
2
3
4
5
6
7
8
Time(s)

Fig.5

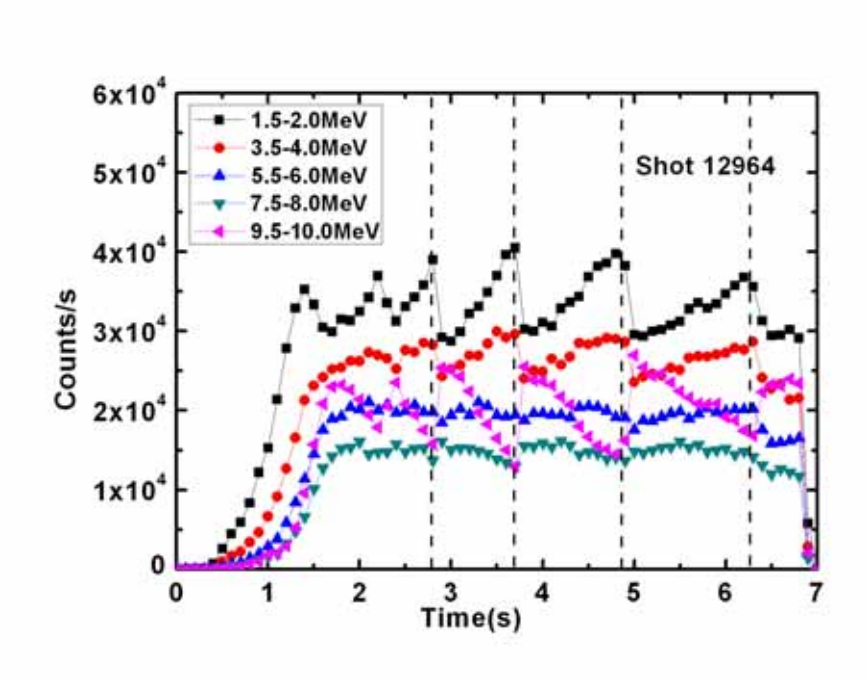
6x10^4
5x10^4
4x10^4
3x10^4
2x10^4
1x10^4
0
Counts/s
0
1
2
3
4
5
6
7
Time(s)
1.5-2.0MeV
3.5-4.0MeV
5.5-6.0MeV
7.5-8.0MeV
9.5-10.0MeV
Shot 12964

Fig.6

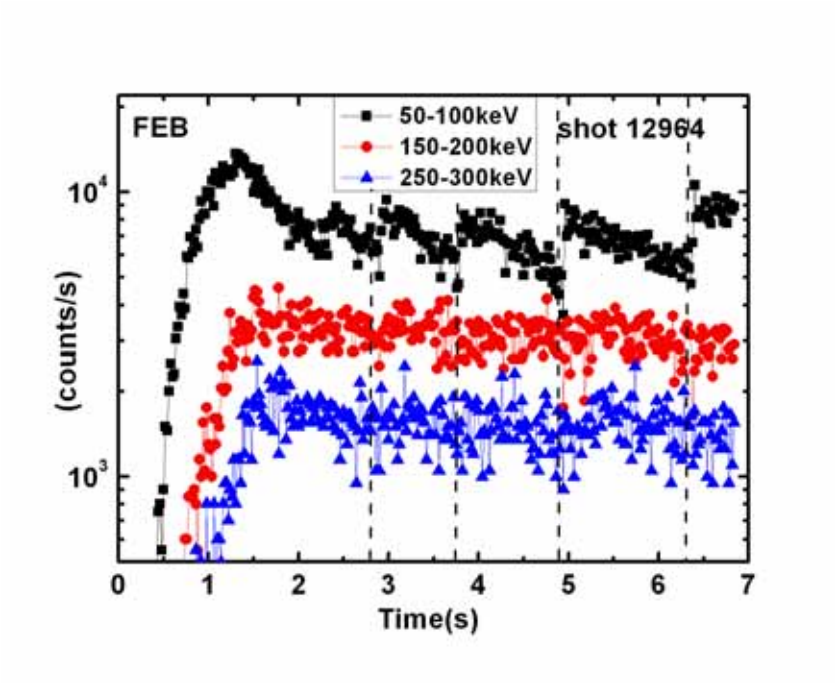
FEB
50-100keV
150-200keV
250-300keV
shot 12964
(counts/s)
10^4
10^3
0
1
2
3
4
5
6
7
Time(s)

Fig.7

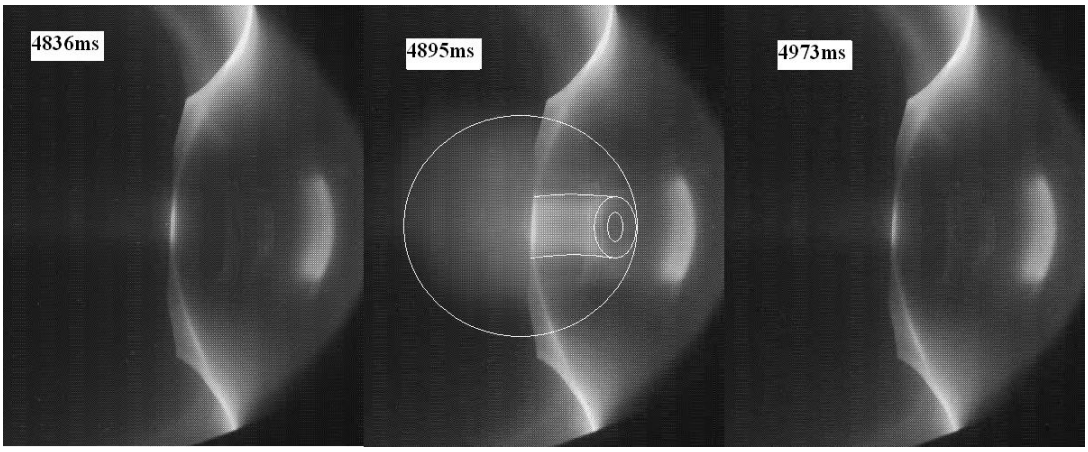

Fig.8